

Dear Author,

Here are the proofs of your article.

- You can submit your corrections **online**, via **e-mail** or by **fax**.
- For **online** submission please insert your corrections in the online correction form. Always indicate the line number to which the correction refers.
- You can also insert your corrections in the proof PDF and **email** the annotated PDF.
- For fax submission, please ensure that your corrections are clearly legible. Use a fine black pen and write the correction in the margin, not too close to the edge of the page.
- Remember to note the **journal title**, **article number**, and **your name** when sending your response via e-mail or fax.
- **Check** the metadata sheet to make sure that the header information, especially author names and the corresponding affiliations are correctly shown.
- **Check** the questions that may have arisen during copy editing and insert your answers/ corrections.
- **Check** that the text is complete and that all figures, tables and their legends are included. Also check the accuracy of special characters, equations, and electronic supplementary material if applicable. If necessary refer to the *Edited manuscript*.
- The publication of inaccurate data such as dosages and units can have serious consequences. Please take particular care that all such details are correct.
- Please **do not** make changes that involve only matters of style. We have generally introduced forms that follow the journal's style. Substantial changes in content, e.g., new results, corrected values, title and authorship are not allowed without the approval of the responsible editor. In such a case, please contact the Editorial Office and return his/her consent together with the proof.
- If we do not receive your corrections **within 48 hours**, we will send you a reminder.
- Your article will be published **Online First** approximately one week after receipt of your corrected proofs. This is the **official first publication** citable with the DOI. **Further changes are, therefore, not possible.**
- The **printed version** will follow in a forthcoming issue.

Please note

After online publication, subscribers (personal/institutional) to this journal will have access to the complete article via the DOI using the URL: [http://dx.doi.org/\[DOI\]](http://dx.doi.org/[DOI]).

If you would like to know when your article has been published online, take advantage of our free alert service. For registration and further information go to: <http://www.link.springer.com>.

Due to the electronic nature of the procedure, the manuscript and the original figures will only be returned to you on special request. When you return your corrections, please inform us if you would like to have these documents returned.

Metadata of the article that will be visualized in OnlineFirst

ArticleTitle	Using indices of atmospheric circulation to refine southern Australian winter rainfall climate projections	
Article Sub-Title		
Article CopyRight	Springer-Verlag GmbH Germany, part of Springer Nature (This will be the copyright line in the final PDF)	
Journal Name	Climate Dynamics	
Corresponding Author	Family Name	Grose
	Particle	
	Given Name	Michael R.
	Suffix	
	Division	
	Organization	CSIRO Climate Science Centre, Oceans and Atmosphere
	Address	Hobart, TAS, Australia
	Phone	
	Fax	
	Email	Michael.Grose@csiro.au
	URL	
	ORCID	http://orcid.org/0000-0001-8012-9960
Author	Family Name	Foster
	Particle	
	Given Name	Scott
	Suffix	
	Division	
	Organization	CSIRO Data61
	Address	Hobart, TAS, Australia
	Phone	
	Fax	
	Email	
	URL	
	ORCID	
Author	Family Name	Risbey
	Particle	
	Given Name	James S.
	Suffix	
	Division	
	Organization	CSIRO Climate Science Centre, Oceans and Atmosphere
	Address	Hobart, TAS, Australia
	Phone	
	Fax	
	Email	
	URL	

ORCID

Author	Family Name	Osbrough
	Particle	
	Given Name	Stacey
	Suffix	
	Division	
	Organization	CSIRO Climate Science Centre, Oceans and Atmosphere
	Address	Aspendale, VIC, Australia
	Phone	
	Fax	
	Email	
	URL	
	ORCID	

Author	Family Name	Wilson
	Particle	
	Given Name	Louise
	Suffix	
	Division	
	Organization	Bureau of Meteorology
	Address	Docklands, VIC, Australia
	Phone	
	Fax	
	Email	
	URL	
	ORCID	

Schedule	Received	13 March 2019
	Revised	
	Accepted	24 June 2019

Abstract

Persistent shifts in mean rainfall have wide-ranging impacts to hydrology and water availability, and a reliable set of climate projections of change to mean rainfall is a useful tool for future planning. Most climate models project a decrease in winter rainfall in southern Australia, however there is a wide model range and there is not yet a robust assessment of underlying physical processes that can inform and constrain projections. Here, a multiple linear regression model between indices of atmospheric circulation and gridded rainfall in observations and in CMIP5 climate models is developed for July, representing the peak of winter. The regression is used as an evaluation tool for models and a basis to select models. Spatial distributions of the coefficients from the regression illustrate the relative importance of different circulation features for rainfall across the region, and illustrate where climate models have deficiencies. As an additional check of projections, historical years that are an analogue for the projected future mean state of the atmospheric circulation are identified and the rainfall anomaly during those years is examined. Both approaches broadly agree and support previous work in suggesting a constraint on rainfall change to a decrease only. The regression analysis also suggests that the median projection for southwest Western Australia should be revised lower than the median of all climate models. The results demonstrate value in applying statistical techniques to understand relationships of rainfall to circulation and to refine confidence in regional climate projections.

Keywords (separated by '-') Atmospheric circulation - Climate projections - Model selection

Footnote Information **Electronic supplementary material** The online version of this article (<https://doi.org/10.1007/s00382-019-04880-4>) contains supplementary material, which is available to authorized users.



2 Using indices of atmospheric circulation to refine southern Australian 3 winter rainfall climate projections

4 Michael R. Grose¹ · Scott Foster² · James S. Risbey¹ · Stacey Osbrough³ · Louise Wilson⁴

5 Received: 13 March 2019 / Accepted: 24 June 2019
6 © Springer-Verlag GmbH Germany, part of Springer Nature 2019

7 Abstract

8 Persistent shifts in mean rainfall have wide-ranging impacts to hydrology and water availability, and a reliable set of climate
9 projections of change to mean rainfall is a useful tool for future planning. Most climate models project a decrease in winter
10 rainfall in southern Australia, however there is a wide model range and there is not yet a robust assessment of underlying
11 physical processes that can inform and constrain projections. Here, a multiple linear regression model between indices of
12 atmospheric circulation and gridded rainfall in observations and in CMIP5 climate models is developed for July, representing
13 the peak of winter. The regression is used as an evaluation tool for models and a basis to select models. Spatial distributions
14 of the coefficients from the regression illustrate the relative important of different circulation features for rainfall across the
15 region, and illustrate where climate models have deficiencies. As an additional check of projections, historical years that
16 are an analogue for the projected future mean state of the atmospheric circulation are identified and the rainfall anomaly
17 during those years is examined. Both approaches broadly agree and support previous work in suggesting a constraint on
18 rainfall change to a decrease only. The regression analysis also suggests that the median projection for southwest Western
19 Australia should be revised lower than the median of all climate models. The results demonstrate value in applying statisti-
20 cal techniques to understand relationships of rainfall to circulation and to refine confidence in regional climate projections.

21 **Keywords** Atmospheric circulation · Climate projections · Model selection

22 1 Introduction

23 A warming climate holds important implications for changes
24 to hydrology and water availability. Persistent shifts in
25 atmospheric circulation and the associated regional rainfall
26 are linked with major impacts to natural and human systems,
27 and changes to circulation due to increased greenhouse gases
28 are less certain than other effects linked to thermodynamic

changes. Circulation change is a major driver of rainfall 29
variability and change in the mid-latitudes in cool seasons, 30
including jets and storm tracks (Hoskins and Valdes 1990; 31
Frederiksen and Frederiksen 2007), baroclinic instability 32
(Phillips 1951) and coherent blocking (Frederiksen and 33
Webster 1988; O’Kane et al. 2013). For southern Australia, 34
rainfall variability and change is primarily a response to 35
changes to rainfall associated with fronts and cutoff lows, 36
arising from changes in storm tracks and blocking regions 37
(Risbey et al. 2013a, b). External anthropogenic forcing is 38
likely to have driven a shift in circulation and rainfall in 39
the cool season in southern Australia (e.g. Frederiksen et al. 40
2017), and further forcing is likely to drive further changes 41
in circulation and rainfall (e.g. Frederiksen and Grainger 42
2015). Changes to convective rainfall may be important to 43
the future rainfall change in summer (e.g. Grose et al. 2019). 44
It would be useful to users of future climate change projec- 45
tions if an analysis of the circulation drivers in models could 46
be used to quantify the confidence in the projections, and 47
ideally to refine the projections including a narrower range 48
of plausible projected change than is currently given. 49

A1 **Electronic supplementary material** The online version of this
A2 article (<https://doi.org/10.1007/s00382-019-04880-4>) contains
A3 supplementary material, which is available to authorized users.

A4 ✉ Michael R. Grose
A5 Michael.Grose@csiro.au

A6 ¹ CSIRO Climate Science Centre, Oceans and Atmosphere,
A7 Hobart, TAS, Australia

A8 ² CSIRO Data61, Hobart, TAS, Australia

A9 ³ CSIRO Climate Science Centre, Oceans and Atmosphere,
A10 Aspendale, VIC, Australia

A11 ⁴ Bureau of Meteorology, Docklands, VIC, Australia

50 The national climate projections for Australia (CSIRO
51 and Bureau of Meteorology 2015) indicate that southern
52 Australia is projected to become drier this century with
53 *high confidence*, based on various lines of evidence includ-
54 ing physical processes, past trends and climate model agree-
55 ment. The projected change is primarily through a decrease
56 in the cooler season rainfall, but with a seasonal and regional
57 signature, including greater decrease centred in winter in
58 southwest Western Australia and a smaller decrease centred
59 in spring in the southeast Australia (Hope et al. 2015).
60 Drying is projected under all Representative Concentra-
61 tion Pathways (RCPs) of van Vuuren et al. (2011), with
62 the greatest reduction under the highest RCP8.5. Using the
63 Coupled Model Inter-comparison Project phase 5 (CMIP5)
64 multi-model database (Taylor et al. 2012) as a primary
65 input, projected change for winter (June, July and August)
66 in the Southern region for 1986–2005 to 2081–2100 under
67 RCP8.5 has a median of -17% and a 10–90 percentile range
68 of -32% to -2% , but the full range of 42 CMIP5 models
69 considered in the national climate projections are noted as
70 possible (-37% to $+1\%$), and the possibility of change out-
71 side this range due to deeper uncertainty is noted.

72 Climate models have biases and some of these biases
73 may affect their projections of climate change (Flato et al.
74 2013). Previous studies propose that some models may be
75 unsuitable or should have a low weighting for some ques-
76 tions or generating particular projections, and the national
77 climate projections discourages certain models to be used as
78 a representative ‘climate futures’ in applications (Whetton
79 et al. 2012). In addition, CMIP5 is an “ensemble of oppor-
80 tunity”, not a true statistical sample of uncertainty, so model
81 independence needs to be accounted for in generating an
82 ensemble. Model selection and weighting is an entire field of
83 research [see studies such as Knutti et al. (2017) and Sander-
84 son et al. (2017)]. There is currently no standard method of
85 evaluating models and applying model weightings to gener-
86 ate climate projections of both the central estimate and
87 range, and different regions have different relevant climate
88 features that affect projected change. Identifying a relation-
89 ship between bias and projected change in particular climate
90 features, known as a process-based emergent constraint, is
91 one of the most promising ways to use evaluation to inform
92 and constrain projections (Eyring et al. 2019). A previous
93 study (Grose et al. 2017) focussed on emergent constraints
94 on rainfall based on atmospheric circulation indices for the
95 southern Australian domain.

96 Atmospheric circulation is a crucial driver of winter
97 rainfall change for southern Australia. Grose et al. (2017)
98 outlined how under ongoing high greenhouse gas emissions,
99 the maximum of baroclinic instability, the storm track and
100 atmospheric jets in the subtropical jet region over Australia
101 are projected to weaken and/or move further south, consist-
102 ent with other work (e.g. Frederiksen and Grainger 2015).

103 Atmospheric blocking is projected to become less frequent
104 and for the peak of blocking in the south Pacific Ocean to
105 possibly move further east, also consistent with previous
106 work (e.g. Parsons et al. 2016; Woollings et al. 2018). As a
107 whole, the study reported that the projection is for a more
108 zonal mean flow with less split flow over eastern Australia
109 and the Tasman Sea in winter. The study found four potential
110 emergent constraints in circulation indices where the bias
111 in the current climate had a relationship to the projected
112 change. These relationships were found in the strength of the
113 subtropical jet, the frequency of blocked days, the longitude
114 of peak blocking frequency and the latitude of the storm
115 track within the polar front jet branch. When outlier mod-
116 els in these constraint relationships were rejected, rainfall
117 projections were constrained at the upper (less dry) end of
118 the projected range in July (from a 10–90% ensemble range
119 of -2 to -28% in CMIP5 to -10 to -32% in the subset).

120 The present study is a follow-up to Grose et al. (2017),
121 and pursues two new methods of using atmospheric circula-
122 tion indices to refine rainfall projections for southern Aus-
123 tralia in winter. The first is the use of a statistical model
124 of rainfall based on circulation indices as a form of model
125 evaluation, the second is the use of circulation indices to
126 identify years in the historical record that are analogues for
127 the future mean (known as temporal analogues).

128 A statistical model of southern Australian rainfall based
129 on atmospheric features can be used as a prediction tool (e.g.
130 Charles et al. 2004; Timbal et al. 2009), which is a specific
131 research field with its own pitfalls (e.g. Fu et al. 2018), and
132 is not the focus here. Rather, we use the comparison of the
133 statistical model generated from observations with that from
134 climate models as a form of evaluating the climate mod-
135 els, then applying this evaluation as a model weighting on
136 the raw model outputs. The temporal analogue approach is
137 closer to statistical downscaling used as prediction mod-
138 els but looks only at monthly mean state rather than daily
139 rainfalls. This approach of using circulation or flow condi-
140 tions as analogues for climatic conditions was suggested as
141 a method to generate climate scenarios in the IPCC third
142 assessment report (Mearns et al. 2001), as used in Wilby
143 et al. (1994). Temporal analogues have also been used in
144 other areas, including to examine extreme heat events (e.g.
145 Jézéquel et al. 2018), assess current mean circulation ana-
146 logues for the mid-Holocene climate (e.g. Antonsson et al.
147 2008), to identify analogues in paleo records that are an
148 analogue for near-term future conditions in Antarctica
149 (Mayewski et al. 2017). Each approach is examined, the
150 similarities and differences are compared, and the results
151 are compared to Grose et al. (2017).

2 Data and methods

2.1 Data

Monthly mean rainfall was taken from the 5×5 km Australian Water Availability Project (AWAP), described in Jones et al. (2009) and Australian Bureau of Meteorology (2019). Gridded data and area averages for the Southern region, as well as Southwest and Southeast sub-regions from the national climate projections were examined (Fig. 1). Circulation indices were calculated from the Japanese Reanalysis JRA55 reanalysis (Kobayashi et al. 2015). The indices are mainly the peak value of the zonal

mean of an atmospheric variable or index such as the jet, baroclinic instability and the storm track across a box over Australia covering the subtropical jet region (90 to 180°E , 10 to 40°S), but some indices use other geographic domains (Table 1). Data were examined for 1958–2005, the start date was chosen as observations are more reliable after 1958, and the end date is chosen to allow comparison to the historical runs of climate models that end in 2005. A multiple linear regression was also fitted to the years in the periods 1958–1980 and 1981–2005, roughly aligning with a change in circulation in the southern hemisphere (Frederiksen and Frederiksen 2007).

Circulation and rainfall were examined in July as a sample of the peak of winter processes (rather than June, July

Fig. 1 Australian region showing box where zonal mean of circulation indices are calculated (dashed), the Southern rainfall region (red), the Southeast sub-region (green); and Southwest sub-region (blue). Vector arrows show the mean wind at 500 hPa in July, reflecting the westerly sub-tropical jet over this region

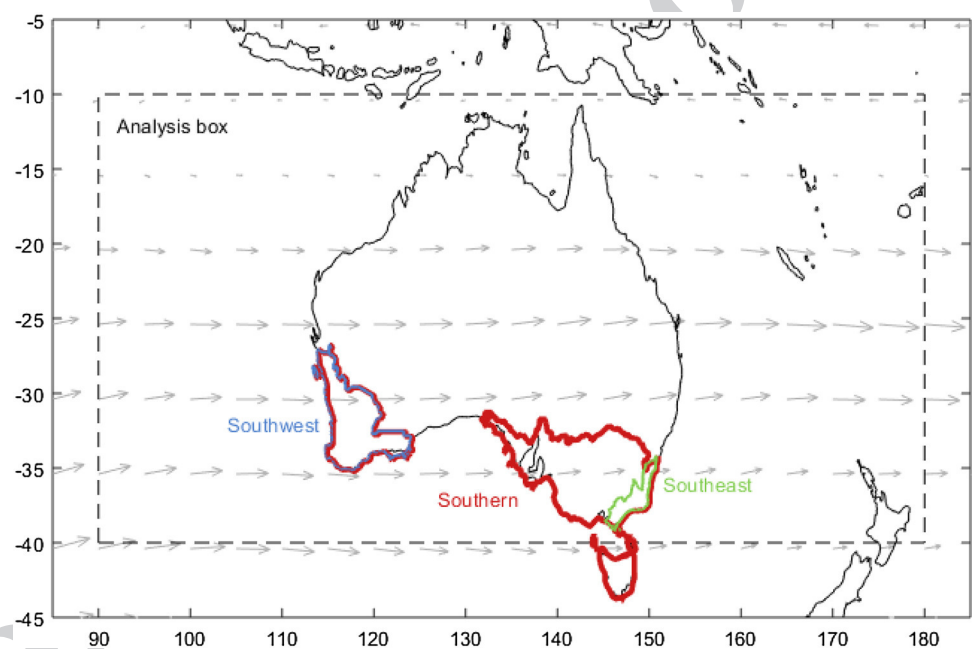


Table 1 Indices of atmospheric circulation relevant to southern Australian rainfall, the mean in 1958–2005 in JRA55, the model mean projected change between 1981–2005 and 2080–2099 from the 26 CMIP5 models

Name	Description	July mean	July projected change
1	PC Peak strength of baroclinic instability as measured by the Philips criterion	19.7	−0.3
2	PC lat. Latitude of the peak in baroclinic instability measured by the Philips criterion	−29.1°S	−1.2°S
3	Jet Peak strength of 300 hPa zonal winds	44.6 m s ^{−1}	−8.4 ms ^{−1}
4	Jet lat. Latitude of the peak in 300 hPa zonal winds	−27.5°S	+0.9°S
5	Storm Peak strength of the storm track (variance in the 500 hPa temperature in the 2–10 day band)	4.9	0 ms ^{−1}
6	Block Frequency of blocking days using the index of Tibaldi and Molteni (1990). For the Southern region, blocking is assessed at 150°E, for regional rainfall blocking was measured at the nearest 10° meridian of longitude	1.1 days	−0.7 days
7	Longitude of peak blocking index east of Australia	170°E	+20°E
8	Latitude of storm track peak	−29.5°S	−0.3°S
9	Peak strength of storm track on the polar front jet (using a box 90 to 180°E, 40 to 70°S)	8.8	+2.1 ms ^{−1}
10	Latitude of storm track on the polar front jet	−58.4°S	+3.1°S

The first six indices are used in evaluating models, the other four are rejected

177 and August). January was examined as the peak of summer
178 in Grose et al. (2017), but is not examined here as there were
179 no emergent constraints found in that season, and other fac-
180 tors than circulation such as convective rainfall change are
181 likely to be important in this season.

182 2.2 Multiple linear regression to evaluate 183 and select climate models

184 A multiple linear regression of inter-annual variations in July
185 rainfall with variations in key circulation indices was per-
186 formed, following the general regression formula in Eq. 1.

$$187 \text{Rainfall}_{i,j} = \beta_0 + \beta_{1,i,j}X_1 + \beta_{2,i,j}X_2 + \dots + \text{Residual}_{i,j} \quad (1)$$

188 where rainfall in a grid cell or region (i, j) is described by
189 an intercept β_0 , and regression coefficients β_k ($k = 1 \dots n$) for
190 that grid cell or region from multiple explanatory variables
191 X_k ($k = 1 \dots n$) that are in this case indices of atmospheric
192 circulation, and the residual.

193 Ten circulation indices described in Grose et al. (2017) are
194 tested here for their ability to describe rainfall within a multi-
195 ple linear regression model (Table 1). These indices quantify
196 the maximum strength (max.) and latitude (lat.) of the baro-
197 clinic instability measured using the Philips criterion (PC),
198 the jet at 300 hPa (Jet), and the storm track (Storm), as well as
199 the frequency and longitude of atmospheric blocking (Block).
200 The mean of these indices in JRA55 in 1958–2005 is shown in
201 Table 1. Each July index for 1958–2005 was detrended using
202 a linear detrend and standardised by removing the mean and
203 dividing by the standard deviation to make the indices, and
204 hence their regression coefficients, commensurate regardless
205 of their initial measurement units. Area-average and gridded
206 rainfall was also detrended using a linear detrend.

207 The multiple linear regression using ten indices (Figure
208 S1) revealed that four indices produced coefficients with
209 rainfall with high values across much of southern and eastern
210 Australia in AWAP/JRA55, so were included (PC, PC lat.,
211 Jet, Jet max.). In addition, two other indices showed notable
212 regional patterns in areas of interest such as the Southeast
213 sub-region or Australian Alps (Storm, Block), and one index
214 produced notable coefficients in the eastern seaboard region
215 (Storm box 2). The other indices (Block lon., Storm lat.,
216 Storm Box 2 lat.) produced coefficients of moderate values
217 in some regions. Since we are fitting to only 48 data points
218 (1959–2005, 48 years) there may be a risk of overfitting the
219 regression, so to help avoid this risk the number of indices
220 were reduced. Models using four and six indices were tri-
221 alled, and the four-index version showed degraded explana-
222 tory power, so the six-index version was used. Indices of Jet
223 and PC indices show some similarity but of opposite sign
224 (coefficient of variation of $R = 0.8$, see Figure S1), but both
225 are included as they aid explanatory power and correlated
226 covariates is not a significant problem for estimation unless

227 multicollinearity is notable. The rejected indices that showed
228 notable coefficients with rainfall in some regions of eastern
229 Australia (Block lon., Storm Box 2) are worth further inves-
230 tigation but are not discussed further here, as the focus is on
231 southern Australia. The regression with six terms is used is
232 used from here on (Eq. 2).
233

$$\begin{aligned} \text{Rainfall}_{i,j} = & \beta_0 + \beta_{1,i,j}\text{PC} + \beta_{2,i,j}\text{PC lat.} + \beta_{3,i,j}\text{Jet} \\ & + \beta_{4,i,j}\text{Jet lat.} + \beta_{5,i,j}\text{Storm} \\ & + \beta_{6,i,j}\text{Block} + \text{Residual}_{i,j} \end{aligned} \quad (2)$$

234 where Rainfall is the rainfall for a grid cell, region or sub-
235 region, and β_k ($k = 1 \dots n$) are the coefficients for each circu-
236 lation index listed in Table 1.

237 The six-factor multiple linear regression was fitted to
238 JRA55 circulation indices and AWAP rainfall data, and then
239 to the simulation of atmospheric circulation and rainfall in
240 CMIP5 global climate models (GCMs). The 26 GCMs that
241 had all indices available were used (Table 2). Rainfall from
242 each GCM is interpolated to a uniform 240×120 global grid
243 (approximately $1.5 \times 1.5^\circ \text{Lat/Lon}$).

244 The coefficients from the multiple linear regression in
245 each CMIP5 model are compared to the coefficients from
246 JRA55/AWAP and the difference is quantified using a nearest
247 neighbour analysis based on the Euclidean distance between
248 the six indices (standardising the indices gives them equal
249 weight). Differences are calculated for area-averaged rain-
250 fall and for each of the GCM grid cells compared to rainfall
251 interpolated to the GCM grid. This Euclidean distance was
252 then used as an evaluation of the models and basis for weight-
253 ing model projections. This approach assumes that the inter-
254 annual variations in circulation and its relation to rainfall
255 is an appropriate analogue for multi-decadal scale changes
256 in circulation and rainfall. Projected change in rainfall for
257 each region was examined for the entire CMIP5 ensemble
258 (42 models), the models tested (26 models), and sub-sets of
259 models based on their Euclidean distance from observations.

260 2.3 Temporal analogue approach

261 The change in rainfall expected from the projected change
262 in atmospheric circulation was explored through a temporal
263 analogue approach. The mean of each index in 1958–2005
264 was calculated in JRA55, and the projected change to each
265 index between 1981–2005 and 2080–2099 was calculated
266 from each GCM (Table 1). The projected GCM change is
267 then simply added to the JRA55 mean to create the analogue
268 of the future mean of these circulation indices (Eq. 3).
269

$$\begin{aligned} \text{Future_mean_analogue} = & (\text{Mean JRA55 1958–2005}) \\ & + (\text{Projected change GCM 1985} \\ & \text{–2005 to 2080–2099, RCP8.5}) \end{aligned} \quad (3)$$

Table 2 CMIP5 global climate models (GCMs) used in this study, the projection of rainfall in the Southern region between 1986–2005 and 2080–2099 under RCP8.5 (Proj), the Euclidean distance of the multiple linear regression from the GCM with JRA55/AWAP in the South-

ern region (Euc Sth), Southeast sub-region (Euc SE) and Southwest sub-region (Euc SW), lowest 6 values are bold, and the projected change in the six atmospheric circulation indices (see Table 1)

	Name	Proj (%)	Euc Sth	Euc SE	Euc SW	PC	PC lat.	Jet	Jet lat.	Storm	Block
1	ACCESS-1.0	-24	19.6	24.0	29.9	-1.6	-1.5	-7.8	0.00	-0.20	-0.52
2	ACCESS-1.3	-24	12.3	39.5	39.4	-0.1	-0.5	-4.0	0.50	0.25	-0.44
3	BCC-CSM1.1	-16	30.7	39.9	50.2	-1.0	-0.9	-3.7	0.25	-0.57	-0.36
4	BCC-CSM1.1-m	-18	34.9	39.1	39.4	0.1	-0.7	-3.2	-1.50	-1.32	-0.12
5	BNU-ESM	-12	12.9	45.1	39.4	0.2	-0.6	-0.2	2.75	-0.19	-0.32
6	CanESM2	-6	14.7	32.5	39.4	-0.6	-2.3	-8.0	-0.50	-0.73	-0.12
7	CMCC-CESM	-21	14.4	50.8	39.4	0.0	0.8	-6.8	8.75	0.37	-0.04
8	CMCC-CM	-28	21.8	26.2	22.0	-0.6	-0.5	-12.2	0.50	0.20	-0.76
9	CMCC-CMS	-21	12.5	28.3	18.5	-1.7	-4.2	-9.7	3.25	0.04	-0.84
10	CNRM-CM5	-24	34.5	61.5	32.0	-0.3	-0.9	-10.9	-0.60	-0.20	-1.08
11	FGOALS-g2	-4	30.3	38.6	39.4	-0.7	-0.8	-8.5	2.50	-0.15	-0.32
12	FGOALS-s2	-2	27.5	35.1	39.4	-0.2	-1.3	-0.1	0.00	0.24	0.00
13	GFDL-CM3	-32	24.1	38.1	24.2	-0.3	-1.8	-5.7	-3.25	0.33	-0.31
14	GFDL-ESM2G	-18	20.3	31.5	39.4	-0.5	-1.8	-10.2	-1.00	0.68	-1.04
15	GFDL-ESM2M	-38	23.6	34.1	39.4	-0.3	-3.5	-10.9	-0.75	0.79	-0.76
16	HadGEM2-CC	-25	30.0	39.7	39.4	-0.9	-2.7	-8.4	-1.50	-0.25	-1.56
17	IPSL-CM5A-LR	-25	11.5	29.6	11.3	-0.1	0.0	-9.4	3.25	1.19	-0.12
18	IPSL-CM5A-MR	-36	7.7	41.0	25.2	0.5	0.9	-11.4	0.50	1.58	-1.36
19	IPSL-CM5B-LR	0	19.9	31.6	27.3	0.0	-0.8	-14.6	3.50	0.15	-1.04
20	MIROC5	-5	41.8	48.6	59.1	0.5	-0.8	-16.5	-1.25	0.11	-2.32
21	MIROC-ESM	-16	24.8	48.7	23.0	-0.8	-1.4	-6.6	5.25	-0.25	-0.12
22	MIROC-ESM-CHEM	-18	15.7	40.4	21.6	0.3	-1.2	-6.4	5.25	-1.15	-0.28
23	MPI-ESM-LR	-7	8.1	25.4	22.3	-0.2	-0.6	-10.4	1.75	-0.16	-1.00
24	MPI-ESM-MR	-30	15.9	33.4	22.6	-1.1	-0.8	-12.1	1.00	0.06	-1.88
25	MRI-CGCM3	-16	19.2	27.6	18.2	0.3	-1.0	-11.6	-0.50	0.13	-1.28
26	NorESM1-M	-5	17.7	39.9	39.4	0.4	-1.4	-8.9	-3.50	-0.36	-0.60
	Multi model mean	-18	21.0	37.3	32.4						

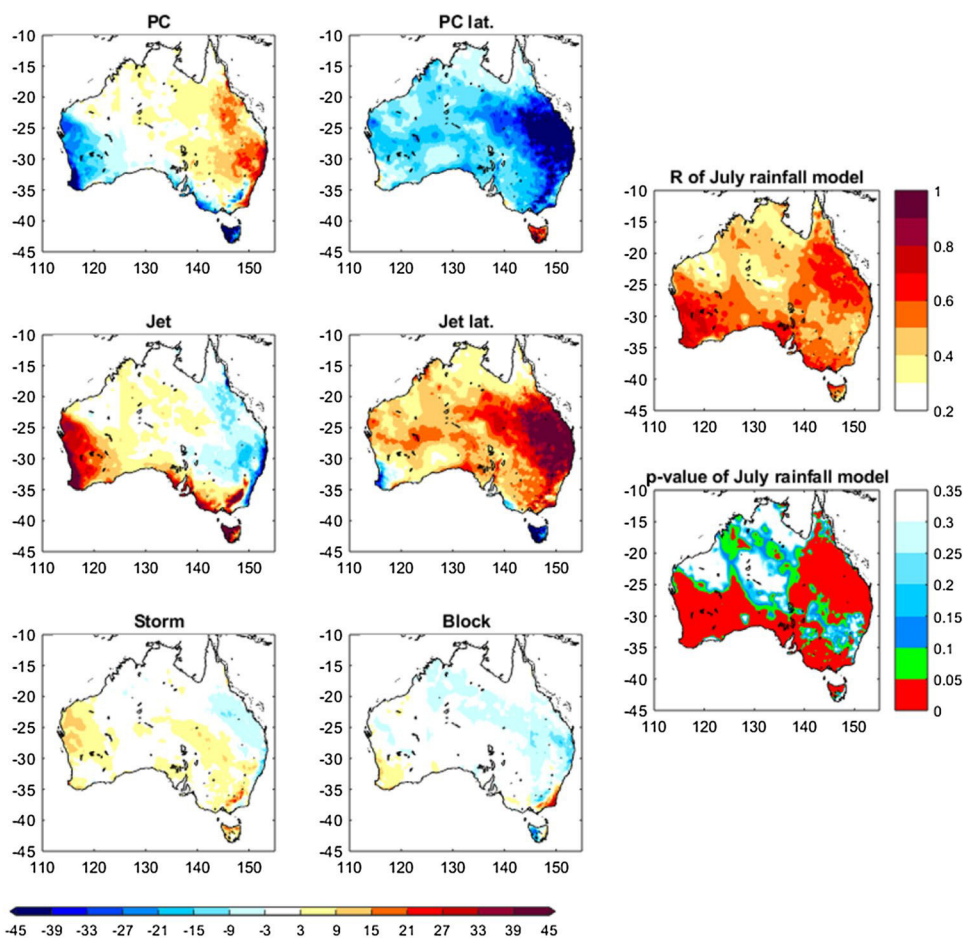
270 For example, the current strength of the Jet is 44.6 ms^{-1} ,
 271 the model mean projected change is -8.4 ms^{-1} , so the
 272 future analogue is 36.3 ms^{-1} . The future mean analogue is
 273 calculated for all six indices for each model and the GCM
 274 mean projection. Indices for all years are standardised by
 275 removing the mean and dividing by the standard deviation,
 276 and this same calibration is applied to the analogue
 277 future mean state. Years in the historical record with the
 278 set of six circulation indices that are most similar to the
 279 analogue future mean of those indices were identified
 280 using the Euclidean distance, then the rainfall anomaly
 281 in the composite of those years is calculated. A sub-set
 282 of 15 years was examined to maintain a relatively small
 283 sample but minimise noise. The rainfall in the 15 analogue
 284 years are then compared to the simulated change in mean
 285 rainfall simulated by the CMIP5 models, and the difference
 286 is calculated.

287 3 Results

288 3.1 Multiple linear regression in JRA55/AWAP

289 Maps of each coefficient from the multiple linear regression
 290 between atmospheric circulation indices in JRA55 and July
 291 rainfall for each cell in AWAP quantify the relationships
 292 with indices across Australia (Fig. 2). These maps reflect
 293 some physically meaningful spatial patterns. For example,
 294 indices associated with westerly circulation such as the
 295 strength of the baroclinic instability (PC) and strength of
 296 the subtropical jet (Jet) produce a high coefficient in areas
 297 such as southwest Western Australia and Tasmania. The sign
 298 reflects the nature of each index, where the strength of the Jet
 299 index is positively related to rainfall, whereas the strength
 300 of PC is inversely related to rainfall. Also, the latitude of
 301 maximum baroclinic instability (PC lat.) and the latitude
 302 of the maximum subtropical jet strength (Jet lat.) have a
 303 high coefficient for eastern Australia and the inland slopes

Fig. 2 Multiple linear regression of six atmospheric circulation indices from JRA55 (see Table 1) and rainfall from each cell of the AAP rainfall dataset in July 1958 to 2005, left: the coefficients of each index (note highest values go off scale), right: the correlation coefficient (R) and p value of the regression in each cell



304 of the Australian Alps, again with opposite sign. Blocking
 305 frequency (Block) has a high positive coefficient over areas
 306 on the southeast coast where it is related to the incidence
 307 of cutoff lows that are associated with higher rainfall, and
 308 a large negative coefficient in western Tasmania where it
 309 relates to lower rainfall due to a blocking of the westerly
 310 flow (Pook et al. 2013). The model has a correlation coef-
 311 ficient (R) over 0.7 and a significance level (p value) under
 312 0.05 for regions of southwest Western Australia, South Aus-
 313 tralia and the coast of southeast Australia. For rainfall aver-
 314 aged over the Southern region, the fit is $R=0.71$.

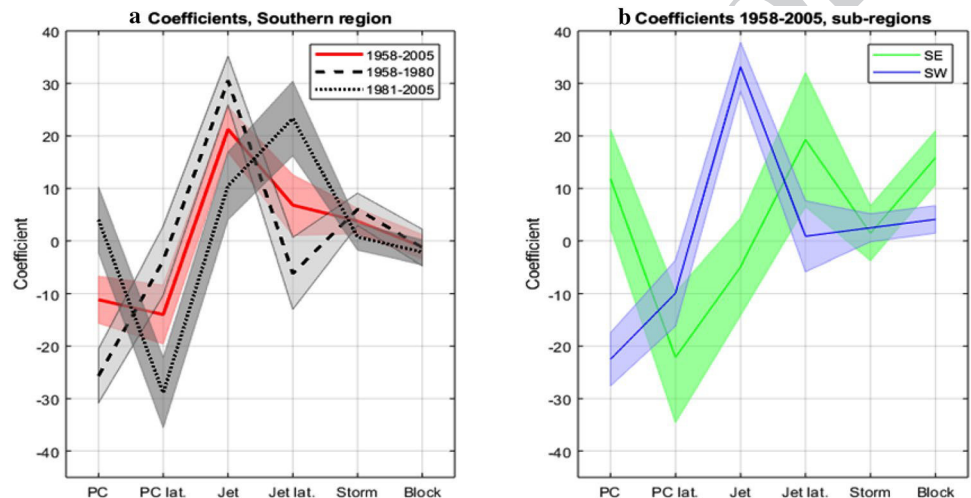
315 The spatial distribution of each coefficients is quite dif-
 316 ferent in the early period 1958–1980 compared to the later
 317 period 1981–2005 (Figure S2), especially the strength of
 318 PC and Jet in eastern Australia, but other instances too.
 319 This suggests the relationship between rainfall and these
 320 circulation indices has changed over time, or that the errors
 321 in reanalyses prior to the satellite era starting in 1979
 322 affect the results, or both. The fit of the statistical model
 323 is also different between the two periods, for the Southern
 324 region, the model has a correlation coefficient of $R=0.7$
 325 for 1958–2005, $R=0.86$ in 1958–1980 and $R=0.74$ in
 326 1981–2005. The cross-sample validation fit is lower, period

327 one model applied to period two $R=0.48$, and period two
 328 model applied to period one $R=0.36$. These fits also suggest
 329 there is a change in the relationship of circulation to rainfall
 330 between the two periods, or there are systematic errors in
 331 observations and reanalyses prior to 1980, or a combina-
 332 tion of both. There is a significant difference in the mean of
 333 the storm track indices (box 1 and box 2) between the two
 334 periods (2-sample t test at the 95% level), but not any other
 335 index.

336 The multiple linear regression for rainfall averaged over
 337 the Southern region (Table 3, Fig. 3a), shows high coeffi-
 338 cients for indices that describe the westerly circulation and
 339 movement of weather systems (PC, Jets). The difference in
 340 the regression in the early period 1958–1980 compared to
 341 the later period 1981–2005 (Fig. 3a) is clear, particularly
 342 the coefficient with PC and Jet latitude. The coefficients are
 343 different for rainfall averaged over the Southeast and South-
 344 west sub-regions (Table 3, Fig. 3b), where the Southeast
 345 sub-region in particular shows stronger relationships with
 346 Block, Jet lat. and PC than the Southwest sub-region, and
 347 the coefficient of PC is of opposite sign. Interestingly, the recent
 348 period for the Southern region shows a stronger relationship
 349 with the Jet lat. and PC than the early period (Fig. 3a), a

Table 3 Coefficients from a multiple linear regression for rainfall averaged over the Southern region, Southeast sub-region and Southwest sub-region with the six circulation indices, standard error is calculated using a 1000 member bootstrap with replacement

		Southern 1958–2005	Southern 1958–1980	Southern 1981–2005	SE 1958–2005	SW 1958–2005
1	PC	-11.1 ± 4.6	-25.8 ± 4.9	4.7 ± 5.8	11.8 ± 10.0	-22.4 ± 4.9
2	PC lat.	-13.3 ± 5.5	-3.4 ± 6.4	-29.5 ± 7.9	-21.8 ± 12.4	-8.3 ± 6.1
3	Jet	20.1 ± 4.6	28.9 ± 4.4	9.9 ± 6.2	-4.9 ± 9.8	30.9 ± 4.8
4	Jet lat.	6.0 ± 5.7	-6.4 ± 6.4	23.6 ± 7.9	18.6 ± 13.0	-0.8 ± 6.3
5	Storm	3.8 ± 2.3	6.3 ± 3.0	0.5 ± 2.6	1.4 ± 4.9	3.4 ± 2.7
6	Block	-1.0 ± 2.3	-1.2 ± 3.4	-2.3 ± 2.5	15.8 ± 5.0	4.3 ± 2.6

Fig. 3 Coefficients from the multiple linear regression for six atmospheric circulation indices in JRA55 (see Table 1) with AWAP for rainfall averaged over Southern region, Southwest sub-region and Southeast sub-region, and different time periods (1958–2005, 1958–1980, 1981–2005) in July. Coloured bands indicate the standard error calculated using a 1000 member bootstrap with replacement

350 pattern more similar to the Southeast sub-region than the
 351 Southwest sub-region (Fig. 3b).

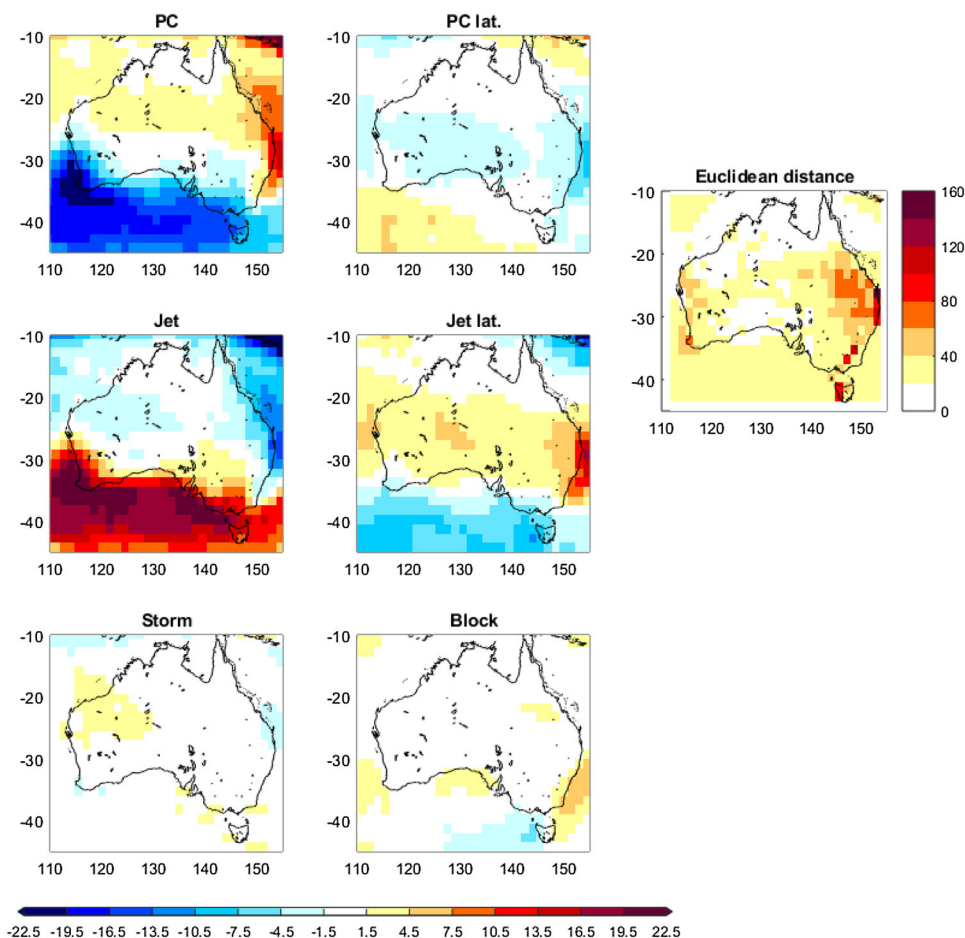
352 3.2 Multiple linear regression in global climate 353 models

354 The spatial distribution of the coefficients from the multiple
 355 linear regression in the mean of 26 climate models (Fig. 4)
 356 shows some broad similarity with that in JRA55/AWAP, but
 357 with lower values. The strength of the Jet and PC have
 358 relatively higher coefficients over the Southern region
 359 including the west coasts, and the coefficient with block-
 360 ing is notable near the southeast coast and Tasmania, but
 361 with lower values than in JRA55/AWAP. Some differences
 362 to observations are related to the coarser resolution, where
 363 mountains, coastlines and the mean position of circulation
 364 features are poorly resolved at the regional scale. This is
 365 illustrated by the Euclidean distance from JRA55/AWAP for
 366 each cell (Fig. 4), where the largest values are found over
 367 mountain and near coastlines. Also, some features unrelat-
 368 ed to resolution appear to be missing in the model mean, such
 369 as the relatively weaker coefficient with the latitude of PC
 370 and jet over the broad region of eastern Australia.

The magnitude of the six coefficients vary between
 models and some models have values more comparable to
 JRA55/AWAP than the model mean, reflected in the coef-
 ficients of the regression for area-averaged rainfall for South-
 ern region and the sub-regions, and the score for the Euclid-
 ean distance scores (Fig. 5). Some persistent biases are seen
 in all models, including a consistently low coefficient for PC
 latitude in the Southern region and Southeast sub-region,
 meaning no model achieves a Euclidean distance from
 JRA55/AWAP below 5 for any region (Fig. 5). The mean of
 the 6 models with the lowest Euclidean distance scores for
 Southern region shows a closer match to JRA55/AWAP than
 the mean of all models, including in the coefficient with PC
 and Jet latitude in eastern Australia (Figure S3).

Using a significance test on the linear fit between Euclid-
 ean distance and the projected change in each circulation
 index (Table 2), there is no significant relationships at the
 95% confidence level. There are three relationships between
 the 90 and 95% confidence level (p value between 0.05 and
 0.1), so are noted as indicative but not significant. The first
 is between Euclidean distance for the Southeast region and
 baroclinic instability (PC) where models with lower Euclid-
 ean distance tend to have a greater decrease in PC (baro-
 clinic instability). This result suggests that models that fit

Fig. 4 Multiple linear regression of six atmospheric circulation indices (see Table 1) and simulated rainfall in July from 26 CMIP5 global climate models (GCMs) in 1958 to 2005, left: multi-model mean of the coefficients with each index (note reduced colour scale compared to Fig. 2, highest values go off scale), right: the Euclidean distance of the six coefficients from the equivalent calculated from JRA55/AWAP (smaller distance denotes a closer match)



395 the circulation-rainfall relationship closer to observations
 396 in the historic climate tend to have a greater sensitivity to
 397 change in baroclinic instability on the climate change scale.
 398 The second is Euclidean distance for the Southern region
 399 rainfall with Jet lat., and the third is Euclidean distance for
 400 the Southern region rainfall with strength of the storm track
 401 (Storm). In these cases, the models with the lower Euclidean
 402 distance tend to show an equatorward movement of Jet lat.
 403 and an increase in Storm track strength.

404 The Euclidean distance is then used as a metric to reject
 405 models for their rainfall projection. There is no significant
 406 linear correlation between any Euclidean distance and any
 407 rainfall projection, therefore there is no emergent constraint
 408 found. However, by first using all models then the subset
 409 of models below percentile values of the range in Euclidean
 410 distance, some constraint of the rainfall projection in
 411 each region appears (Fig. 6). Here, the 75% (19 models),
 412 then 50% (13 models) and then 25% (6 models) thresholds
 413 are used. For the Southern region as a whole, the rainfall
 414 projection becomes constrained at the wetter end and the
 415 median decreases somewhat, a result very similar to Grose
 416 et al. (2017). For the Southeast sub-region, the projected
 417 range becomes reduced when using only the 6 models with

418 the lowest Euclidean distance, particularly the wetter end,
 419 but with little change in the median. For the Southwest sub-
 420 region, the median projection is considerably lower (−10%)
 421 for all sub-groups of models compared to the whole ensemble,
 422 but with only a small change in the model spread.

3.3 Analogue years 423

424 The historical years with circulation indices most similar
 425 to the GCM mean projected climatological mean of those
 426 indices are in order: 1993, 1959, 1992, 1962, 1985, 1976,
 427 1994, 1984, 1969, 1967, 1999, 1988, 1970, 1975 and 1961.
 428 Examining a composite of these 15 years, rainfall was below
 429 average across southern Australia but above average in east-
 430 ern Australia (Fig. 7b). The results are broadly consistent
 431 across all 26 individual models (Figure S4).

432 This spatial distribution of the rainfall anomaly in ana-
 433 logue years (Fig. 7b) is similar to the mean rainfall pro-
 434 jection from CMIP5 in southern Australia (Fig. 7c), but is
 435 quite different in eastern Australia. Area-averaged rainfall
 436 anomaly in the Southern region (−12%) is less dry than
 437 CMIP5 (−18%). Rainfall was below average in the South-
 438 west sub-region in analogue years (−18%), which is less

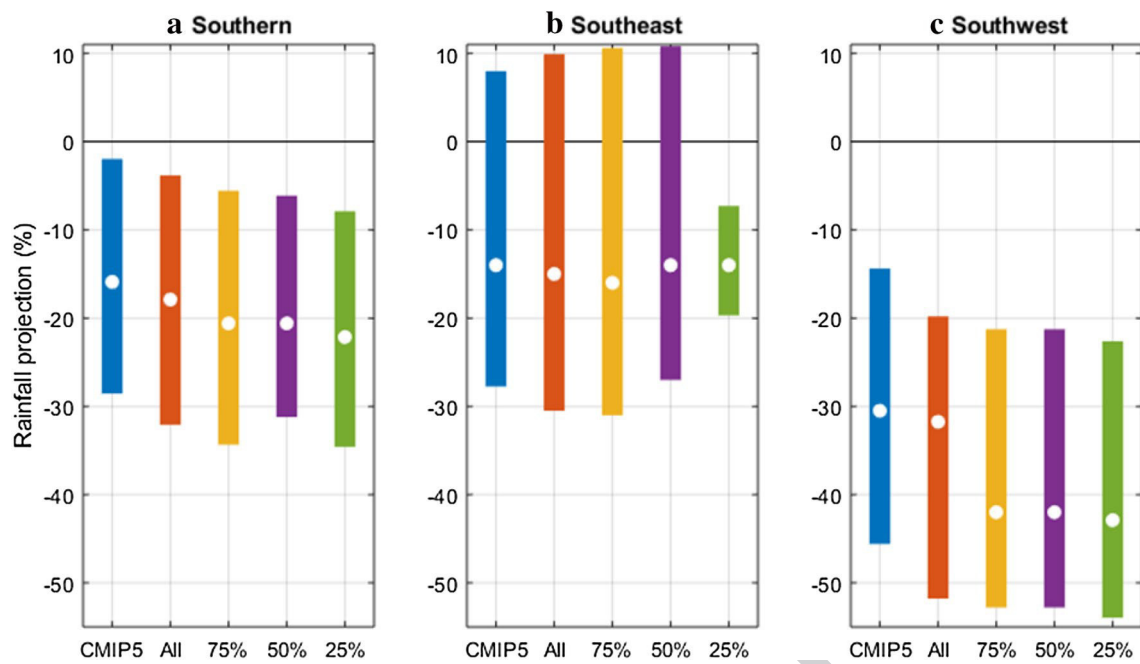


Fig. 6 Rainfall projection for July rainfall between 1986–2005 and 2080–2099 under RCP8.5, bars are the 10–90 percentile range, circle is the median for **a** Southern region, **b** Southeast sub-region, and **c** Southwest sub-region. Series are 42 CMIP5 models (CMIP5), 26

CMIP5 models tested in this study (All), and models with the lowest Euclidean distance from JRA55/AWAP for the relevant region (75%: 19 models, 50%: 13 models, and 25%: 6 models)

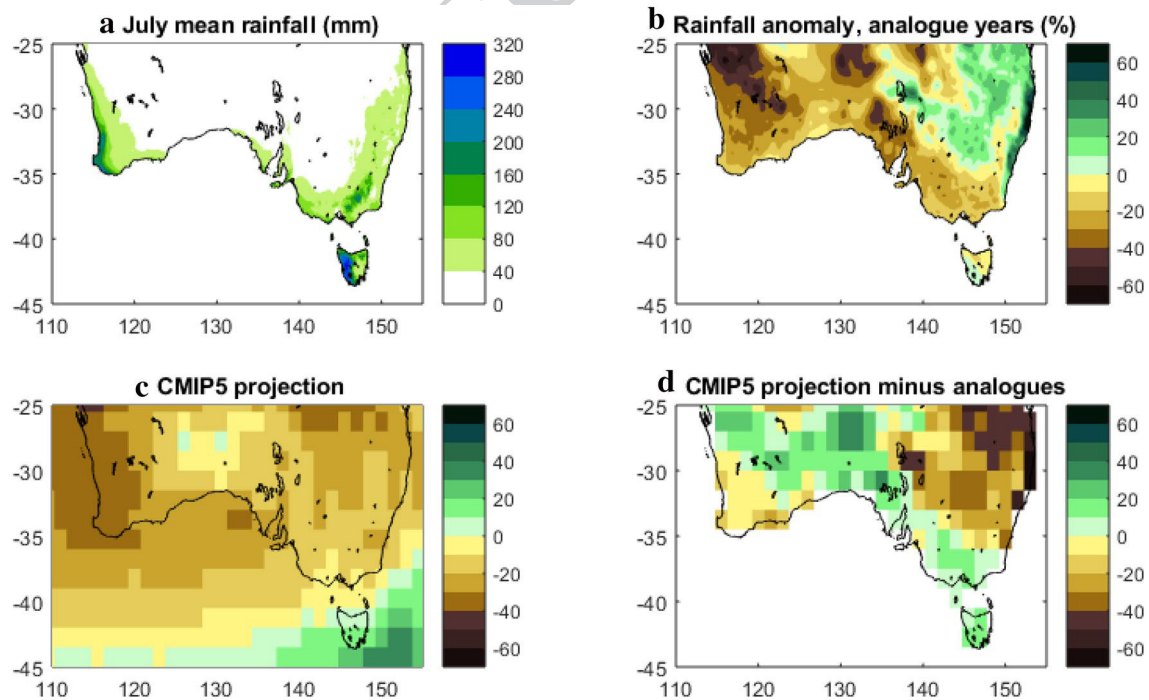


Fig. 7 July rainfall in southern Australia: **a** mean rainfall in July in AWAP in 1958–2005, **b** the anomaly of mean rainfall (%) of the 15 analogue years, **c** mean projection from 26 CMIP5 models tested in

this study for 1986–2005 to 2080–2099 (%), **d** the difference between the CMIP5 projection and the 15 analogue years (%)

451 Rainfall was above average in southwestern Tasmania (by
452 up to 23%).

453 If we assume this composite of analogue years as an esti-
454 mate of the projected change in rainfall due to changes in
455 atmospheric circulation, and that CMIP5 gives an accurate
456 projection of all factors driving rainfall change, then the
457 difference between the analogue years and the total projec-
458 tion from CMIP5 (Fig. 7d) is an estimate of the change due
459 to non-circulation processes such as the effect of a warmer
460 atmosphere. This difference suggests that the non-circulation
461 factors offset circulation-driven drying in the broad south-
462 east Australian region and Tasmania, enhance the drying of
463 southwest western Australia and offset a strong increase in
464 rainfall increase on the eastern seaboard. Alternatively, the
465 difference could suggest where CMIP5 models have defi-
466 ciencies in their simulated response to circulation change,
467 through poor resolution of topography or other factors.

468 4 Discussion

469 This paper presents the results of two different approaches
470 to refining climate projections of southern Australian July
471 rainfall (representing the peak of winter) using indices of the
472 most important driver of projected rainfall change; atmos-
473 pheric circulation change. The agreement between the two
474 methods, and with previous work, provides further evidence
475 for a constraint on the wetter end of winter rainfall projec-
476 tions for rainfall in the Southern region. The results from
477 the two approaches give some different projections for the
478 sub-regions of southern Australia.

479 The first analysis uses a multiple linear regression of
480 inter-annual rainfall variability based on circulation indi-
481 ces as a form of model evaluation. A comparison of the
482 regression of rainfall related to circulation indices tests
483 the relationship between the atmospheric circulation and
484 regional rainfall on a year-to-year basis. This represents an
485 integrated assessment of six important indices in a single
486 metric, so is less vulnerable to arbitrary choices of indices
487 and their weighting. This process assumes that it is accept-
488 able to apply an evaluation based on inter-annual variability
489 to projections at the climate change scale, but we note that
490 the relationship between circulation and rainfall is essential
491 to making reliable projections, and the inter-annual rela-
492 tionship is at least some guide to the quality of simulated
493 changes at the climate change scale. Further work could
494 be done to compare the relationships at longer timescales,
495 including decadal or multi-decadal over the historical record.

496 The regression produces quite different results when it
497 is fitted to the periods 1958–1980 and 1981–2005, and this
498 boundary is associated with a reported shift in circulation
499 (Frederiksen and Frederiksen 2007), but also the start of the
500 satellite era and use of remote sensing to inform reanalyses

such as JRA55 (Kobayashi et al. 2015). This suggests that
either there was a change in the relationship between cir-
culation and rainfall at many locations between these two
periods, or there was a notable change in the quality of re-
analysis data at this time, or contributions from both. The lack
of stationarity in the observed relationship between circula-
tion indices and rainfall has implications for making climate
projections, where free-running climate models should not
be expected to exactly match this observed relationship over
a period of a few decades, and the relationship shouldn't be
expected to stay the same in the future. This lack of station-
arity also suggests that analogue-based statistical downscal-
ing methods need to use caution when selecting suitable
calibration periods. Producing a multiple linear regression of
rainfall based on atmospheric circulation indices represents
a novel method to draw out and visualise changes in these
relationships through time, regardless of their cause.

The Euclidean distance between climate models and
observations is larger over areas where GCMs do not resolve
important features such as mountains, which is consistent
with previous findings such as that GCMs do not simulate
the relationship with zonal wind over the Australian Alps
(Pepler et al. 2015), and do not distinguish the regional detail
of rainfall over Tasmania (Corney et al. 2013). The analysis
also shows that most GCMs produce a lower regression coef-
ficient with indices such as the jet latitude than in observa-
tions for a broad region of eastern Australia (not just the
eastern seaboard east of the mountain range). This suggests
that GCMs have biases in the broader scale processes in this
area, providing a barrier to reliable rainfall projections not
just related to the resolution of mountains. This may be a
reason why there is no clear unambiguous 'added value' in
the rainfall change projection through downscaling of GCMs
for the eastern region (Grose et al. 2015). However, given
that the relationships between PC and Jet indices changed
between the two historical periods, the difference between
models and observations may be due partly to natural vari-
ability rather than model bias.

To apply the evaluation to constrain projections, it would
be useful if there were relationships between the Euclidean
distance and projected change of either the circulation indi-
ces or rainfall. There were some indicative but not signifi-
cant relationships between Euclidean distance and projection
of circulation indices, but these relationships do not build
a simple and consistent picture to constrain projections of
circulation change. There were no significant relationships
across the spread of models in Euclidean distance and rain-
fall projections, so there are no emergent constraints found
there. However, by accepting or rejecting models based
on their distances then some constraints become apparent.
For the Southern region, the models with a closer match to
observations are constrained at the wetter end compared to
the whole CMIP5 ensemble, meaning that there is higher

554 agreement on significant drying than the whole ensemble.
 555 Also, the models with a lower Euclidean distance showed a
 556 lower median projection for the Southwest sub-region than
 557 the whole ensemble by around 10%. This is physically plau-
 558 sible, and broadly consistent with a previous study (Grose
 559 et al. 2017) that looked at emergent constraints on the indi-
 560 ces themselves.

561 The second analysis used temporal analogues to show
 562 the ensemble mean projection of circulation features and
 563 produces results broadly consistent with rainfall projec-
 564 tions from CMIP5. Temporal analogues calculated from
 565 each model and the model mean were broadly consistent.
 566 This supports circulation changes as the dominant driver
 567 of rainfall change in southern Australia in general, and that
 568 CMIP5 models simulate the relationship between change
 569 in circulation and rainfall in a similar pattern as observa-
 570 tions. There is a difference between the temporal analogues
 571 and the CMIP5 projection, where CMIP5 is less dry in the
 572 Southeast sub-region and drier in the Southwest sub-region
 573 than the analogue years. This suggests that either CMIP5 has
 574 a bias in the rainfall projection associated with this circula-
 575 tion change, including an underestimate of the drying in the
 576 southeast, or that projected changes unrelated to these cir-
 577 culation indices are offsetting the effect. These other factors
 578 may include thermodynamic changes or other forcings such
 579 as the lifting of the anthropogenic aerosol burden. Alterna-
 580 tively, some or all of the differences may be due to errors in
 581 the CMIP5 models, or else noise in the sample of 15 years to
 582 generate the analogues. Large differences between the tem-
 583 poral analogue and CMIP5 in the eastern seaboard region
 584 are worth further investigation.

585 As well as examining the multiple linear regression as
 586 an evaluation over longer timeframes such as decadal vari-
 587 ability, further work could include applying the model to
 588 other seasons, other places, and comparing the results to
 589 statistical downscaling. The multiple linear regression could
 590 include changes to temperature and humidity to model the
 591 change in rainfall incorporating thermodynamic as well as
 592 dynamic aspects of rainfall change in an integrated way.
 593 Similarly, the simple circulation analogue approach could
 594 also be compared to the results from other sophisticated sta-
 595 tistical models of daily rainfall that use circulation and other
 596 atmospheric analogues as input.

597 5 Conclusions

598 The results presented here support constraining the wet end
 599 of rainfall projections for the Southern region from CMIP5,
 600 giving higher agreement and confidence in a drying climate
 601 in southern Australia due to climate change than CMIP5
 602 suggests. This means that a projection of little change or a
 603 slight increase in rainfall in the Southern region, suggested

604 by some CMIP5 members, should be given less confidence
 605 than projections in the rest of the model range. The meth-
 606 ods demonstrate a further physical basis for informing the
 607 projected change in rainfall for regions where circulation
 608 indices are important, further to Grose et al. (2017).

609 The results from the two approaches differ regarding
 610 the projection for sub-regions of southern Australia. The
 611 model rejection analysis suggests a 10% drier median rain-
 612 fall projection for the Southwest sub-region than the entire
 613 CMIP5 ensemble for the end of the century under a high
 614 emissions scenario. The temporal analogue analysis suggests
 615 a slightly wetter median projection for the southwest but a
 616 drier projection for the broad southeast Australian region
 617 than CMIP5 projects.

618 The results suggest that the use of a statistical model of
 619 rainfall based on atmospheric circulation indices has utility
 620 beyond prediction, through use as an evaluation method and
 621 tool to examine physical relationships between rainfall and
 622 circulation.

623 **Acknowledgements** This work was supported by the Australian Gov-
 624 ernment's National Environmental Science Program (NESP) Earth
 625 System and Climate Change (ESCC) hub. We acknowledge the World
 626 Climate Research Programme's Working Group on Coupled Model-
 627 ling, which is responsible for CMIP, and we thank the climate model-
 628 ling groups for producing and making available their model output.
 629 James Risbey is supported by the CSIRO Decadal Climate Forecasting
 630 Project.

631 References

- 632 Antonsson K, Chen D, Seppä H (2008) Anticyclonic atmospheric cir-
 633 culation as an analogue for the warm and dry mid-Holocene sum-
 634 mer climate in central Scandinavia. *Clim Past* 4:215–224
 635 Australian Bureau of Meteorology (2019) Australian Gridded Climate
 636 Data (AGCD)/AWAP; v1.0.0 Snapshot (1900-01-01 to 2018-12-
 637 31) <https://doi.org/10.4227/166/5a8647d1c23e0>
 638 Charles SP, Bates B, Smith IN, Hughes JP (2004) Statistical down-
 639 scaling of daily precipitation from observed and modelled atmos-
 640 pheric fields. *Hydrol Process* 18:1373–1394
 641 Corney SP, Grose MR, Bennett JC, White CJ, Katzfey JJ, McGregor
 642 JL, Holz GK, Bindoff NL (2013) Performance of downscaled
 643 regional climate simulations using a variable-resolution regional
 644 climate model: Tasmania as a test case. *J Geophys Res Atmos*
 645 118:1–15
 646 CSIRO and Bureau of Meteorology (2015) Climate Change in Aus-
 647 tralia, Technical Report. Melbourne, Australia. www.climatechangeinaustralia.gov.au
 648 Eyring V et al (2019) Taking climate model evaluation to the next level.
 649 *Nat Climate Change*. <https://doi.org/10.1038/s41558-018-0355-y>
 650 Flato G et al (2013). Evaluation of climate models. In: Stocker TF,
 651 Qin D, Plattner G-K et al (eds) *Climate change 2013: the physical
 652 science basis. Contribution of working group I to the fifth assess-
 653 ment report of the intergovernmental panel on climate change*.
 654 Cambridge University Press, Cambridge, pp 741–866. [https://doi.
 655 org/10.1017/CBO9781107415324.020](https://doi.org/10.1017/CBO9781107415324.020)
 656 Frederiksen JS, Frederiksen CS (2007) Interdecadal changes in south-
 657 ern hemisphere winter storm track modes. *Tellus* 59:599–617
 658

- 659 Frederiksen CS, Grainger S (2015) The role of external forcing in
660 prolonged trends in Australian rainfall. *Clim Dyn* 45:2455–2468
- 661 Frederiksen JS, Webster PJ (1988) Alternative theories of atmospheric
662 teleconnections and low-frequency fluctuations. *Rev Geophys*
663 26:459–494
- 664 Frederiksen CS, Frederiksen JS, Sisson JM, Osbrough SL (2017)
665 Trends and projections of Southern Hemisphere baroclinicity: the
666 role of external forcing and impact on Australian rainfall. *Clim*
667 *Dyn* 48:3261–3282
- 668 Fu G, Charles SP, Chiew FHS, Ekström M, Potter NJ (2018) Uncertain-
669 ties of statistical downscaling from predictor selection: equifinal-
670 ity and transferability. *Atmos Res* 203:130–140
- 671 Grose MR, Bhend J, Argueso D, Ekström M, Dowdy AJ, Hoffmann P,
672 Evans JP, Timbal B (2015) Comparison of various climate change
673 projections of eastern Australian rainfall. *Aust Meteorol Oceanogr*
674 J 65:72–89
- 675 Grose MR, Risbey JS, Moise AF, Osbrough S, Heady C, Wilson
676 L, Erwin T (2017) Constraints on Southern Australian rainfall
677 change based on atmospheric circulation in CMIP5 simulations.
678 *J Clim* 30:225–242
- 679 Grose MR, Syktus J, Thatcher M, Evans JP, Ji F, Rafter T, Remenyi
680 T (2019) The role of topography on projected rainfall change in
681 mid-latitude mountain regions. *Clim Dyn*. [https://doi.org/10.1007/
682 s00382-019-04736-x](https://doi.org/10.1007/s00382-019-04736-x)
- 683 Hope PK et al (2015) Seasonal and regional signature of the projected
684 southern Australian rainfall reduction. *Aust Meteorol Oceanogr*
685 J 65:54–71
- 686 Hoskins BJ, Valdes PJ (1990) On the existence of storm-tracks. *J*
687 *Atmos Sci* 47:1854–1864
- 688 Jézéquel A, Yiou P, Radanovics S (2018) Role of circulation in Euro-
689 pean heatwaves using flow analogues. *Clim Dyn* 50:1145–1159
- 690 Jones DA, Wang W, Fawcett R (2009) High-quality spatial climate
691 data-sets for Australia. *Aust Meteorol Oceanogr* J 58:233–248
- 692 Knutti R, Sedláček J, Sanderson BM, Lorenz R, Fischer EM, Eyring
693 V (2017) A climate model projection weighting scheme account-
694 ing for performance and interdependence. *Geophys Res Lett*
695 44:1909–1918
- 696 Kobayashi S et al (2015) The JRA-55 reanalysis: general specifications
697 and basic characteristics. *J Meteorol Soc Jpn Ser II* 93:5–48
- 698 Mayewski PA et al (2017) Ice core and climate reanalysis analogs to
699 predict Antarctic and Southern Hemisphere climate changes. *Quat*
700 *Sci Rev* 155:50–66
- 701 Mearns LO, Hulme M, Carter TR, Leemans R, Lal M, Whetton PH
702 (2001) Climate scenario development. In: Houghton J et al (eds)
703 IPCC third assessment report. The science of climate change.
704 Cambridge University Press, Cambridge, pp 739–768
- 705 O’Kane TJ, Risbey JS, Franzke C, Horenko I, Monselesan DP
706 (2013) Changes in the metastability of the midlatitude southern
hemisphere circulation and the utility of nonstationary cluster
analysis and split-flow blocking indices as diagnostic tools. *J*
Atmos Sci 70:824–842
- Parsons S, Renwick JA, McDonald AJ (2016) An assessment of future
southern hemisphere blocking using CMIP5 projections from four
GCMs. *J Clim* 29:7599–7611
- Pepler A, Alexander L, Evans J, Sherwood S (2015) Zonal winds and
southeast Australian rainfall in global and regional climate mod-
els. *Clim Dyn*. <https://doi.org/10.1007/s00382-015-2573-6>
- Phillips NA (1951) A simple three-dimensional model for the study
of large-scale extratropical flow patterns. *J Meteorol* 8:381–394
- Pook MJ, Risbey JS, McIntosh PC, Ummenhofer CC, Marshall AG,
Meyers GA (2013) The seasonal cycle of blocking and associated
physical mechanisms in the Australian region and relationship
with rainfall. *Mon Weather Rev* 141:4534–4553
- Risbey JS, McIntosh PC, Pook MJ (2013a) Synoptic components of
rainfall variability and trends in southeast Australia. *Int J Climatol*
33:2459–2472
- Risbey JS, Pook MJ, McIntosh PC (2013b) Spatial trends in synoptic
rainfall in southern Australia. *Geophys Res Lett* 40:3781–3785
- Sanderson BM, Wehner M, Knutti R (2017) Skill and independence
weighting for multi-model assessments. *Geosci Model Dev*
10:2379–2395
- Taylor KE, Stouffer RJ, Meehl GA (2012) An overview of CMIP5 and
the experiment design. *Bull Am Meteorol Soc* 93:485–498
- Tibaldi S, Molteni F (1990) On the operational predictability of block-
ing. *Tellus A* 42:343–365
- Timbal B, Fernandez E, Li Z (2009) Generalization of a statistical
downscaling model to provide local climate change projections
for Australia. *Environ Model Softw* 24:341–358
- van Vuuren D et al (2011) The representative concentration pathways:
an overview. *Clim Change* 109:5–31
- Whetton P, Hennessy K, Clarke J, McInnes K, Kent D (2012) Use of
representative climate futures in impact and adaptation assess-
ment. *Clim Change* 115:433–442
- Wilby R, Greenfield B, Glenny C (1994) A coupled synoptic-hydro-
logical model for climate change impact assessment. *J Hydrol*
153:265–290
- Woollings T et al (2018) Blocking and its response to climate change.
Curr Clim Change Rep 4:287–300
- Publisher’s Note** Springer Nature remains neutral with regard to
jurisdictional claims in published maps and institutional affiliations.

Journal:	382
Article:	4880

Author Query Form

Please ensure you fill out your response to the queries raised below and return this form along with your corrections

Dear Author

During the process of typesetting your article, the following queries have arisen. Please check your typeset proof carefully against the queries listed below and mark the necessary changes either directly on the proof/online grid or in the 'Author's response' area provided below

Query	Details Required	Author's Response
AQ1	Kindly check and confirm whether the corresponding author and mail id is correctly identified.	